

Experimental and numerical study of the initial stages in the interaction process between a planar shock wave and a water column

Dan Igra and Kazuyoshi Takayama

Shock Wave Research Center, Institute of Fluid Science, Tohoku University, Sendai, Japan 980 - 8577

Abstract. An experimental and numerical study of shock wave loading on a cylindrical water column is presented. Experiments were conducted in a 4 mm x 150 mm shock tube equipped with holographic interferometry. The cylindrical water column had a diameter of 6.4 mm and height of 4 mm. It was exposed to a shock wave of Mach number 1.3 in atmospheric air. Corresponding Weber and Reynolds numbers to these conditions were 3,690 and 95,300, respectively. A numerical scheme was developed based on an upwind TVD scheme. Using this scheme the initial stages of the shock wave interaction with the water column were studied. At these stages a transmitted shock wave propagates inside the water column. The obtained numerical results agreed well with experimental findings.

1 Introduction

The breakup of liquid droplets induced by high speed gas flows has many applications such as damage of rain droplets impinging on aircrafts in supersonic flight, ablation of space vehicles during atmosphere re-entry, combustion and detonation in two-phase mixtures etc. As a result, it has been extensively studied by many researchers. A comprehensive review of droplet breakup can be found in Wierzba and Takayama [9]. Ranger and Nicholls [7] visualized the various stages of the droplet breakup processes using shadowgraph. Recently Joseph et al. [4] conducted a series of experiments, using a high speed camera, where various liquids were impinged by shock waves of Mach numbers 2 and 3. Advantages of double exposure holographic interferometry applied to droplet breakup process, were well demonstrated by Yoshida and Takayama [10]. They have shown that the observed patterns of the droplet breakup differed significantly depending upon the method of visualization. Patterns of droplets disintegration observed by double exposure holographic interferometry, were found to be different from those observed on the unreconstructed holograms, which is essentially equivalent to direct a shadowgraph. Previously, schlieren method or shadowgraph was implemented to visualize the droplet breakup process, in which the shape of disintegrating spherical droplets appeared to be similar to fireball geometry [4, 7]. On these photographs the internal structure of disintegrating spherical droplets such as shattering mist clouds and wakes were hardly visible. However, using holographic interferometry slightly 3D images containing mist clouds and wakes look different from that observed in schlieren photographs and shadowgrams.

Object beams of holographic interferometry carry phase information created by light scattered from micro-mist particles to a holofilm. Through the process of reconstruction, the phase information were partially recovered, whereas in the schlieren method or shadowgraph, these could never be stored on a film.

In all experiments mentioned so far spherical water droplets were employed so that three-dimensional interactions should be visualized. However, three-dimensional visualization is still in the process of development. Therefore a planar shock wave collision with a cylindrical liquid column, which is a two-dimensional droplet can be examined. In order to account for the process of disintegration and particularly to clarify the effect of wave motions inside the droplet, visualization of the interaction of a shock wave with a liquid column is important. The results of visualization could be extended to interpret complex three-dimensional droplet breakup.

Numerical simulation can contribute to this investigation. However water/air two phase flows are difficult to correctly simulate. It is one of the challenging topics of computational fluid dynamics. The main problem lies in modeling the gas/liquid interface. Shock capturing schemes such as TVD or ENO are useful in simulating accurately single component gas flows. However, in the case of multi-components flows, consisting of two phase flows with interfaces, often physically non realistic pressure fluctuations appear across the interfaces. These pressure fluctuations are generated as a result of deriving pressures from the equation of state based on the total energy in the gaseous phase. In multi-component flows, even when densities and velocities of the components are initially identical, the internal energy of individual components will not be identical due to the difference in their specific heats ratios γ , and hence at every time step, energy diffusion occurs across the interface. When the value of γ changes discontinuously across the interface, incorrect pressures value will be obtained at the interface. In the next time step, a false velocity will be derived out of incorrect pressure values. See Karni for details [5]. Karni [5], Cocchi et al. [1] and others proposed possible methods to overcome this problem. In most schemes, the shock wave was typically stretched over 2 - 3 grid points while the interface was smeared over 5 - 7 grid points. This could be acceptable when dealing with a pure gas phase. However, in the case of two-phase flow consisting of gas and liquid phases accompanying very large density difference between the two phases, density diffusion at the interface is strictly unacceptable. Physically interfacial mixing hardly takes place at gas/liquid interfaces except in very special cases. Numerical diffusion might result in unphysical densities at interfaces. Therefore, a different method should be used to overcome this numerical mixing. This method can eliminate pressure fluctuations at the interface and keep a discontinuous density profile at the interface. Cocchi et al. [1] achieved these goals by employing a Godunov scheme coupled with a front tracking method. Their scheme used results derived from the exact Riemann solver at the interface for correcting the density diffusion and pressure fluctuations at the interface by interpolating the results of the exact Riemann solver with grid points that were not affected by diffusion near the interface. The pressure and density are corrected at the grid points across

the interface. Therefore, the numerical density diffusion and pressure oscillations are eliminated. Thus a discontinuous interface is retained for the next iteration.

The numerical scheme developed here is based on an upwind TVD scheme with the correction step described above. The interface is captured using the level set approach of Sethian [8].

2 Numerical scheme

2.1 Level set approach

Mulder et al. [6] presented an ENO scheme incorporating the level set approach to track a two gas interface. It can capture the interface between two grid points. Let the level set function ψ be defined as the distance between a grid point and the interface. $\psi=0$ designates the interface. Then positive ψ designates one material and negative ψ designates another material. Knowing the value of ψ the specific heats ratio can be defined as a function of the level set function.

$$\gamma(\psi) = \begin{cases} \gamma, & \psi > 0 \text{ for gas,} \\ n, & \psi < 0 \text{ for liquid.} \end{cases} \quad (1)$$

The level set function propagates with the local fluid velocity and can be written as the advection equation in non-conservative form.

$$\psi_t + u\psi_x = 0 \quad (2)$$

The location of the interface can be readily found by satisfying the following equation,

$$\psi_i\psi_{i+1} < 0 \quad (3)$$

Where the interface is located between grid points i and $i+1$. Now that the use of the level set approach is explained, it will be incorporated into a system of hyperbolic conservation laws.

2.2 The equation of state

Equations of state for individual components are an essential part of the flow solver. In the simulation of gas/liquid interface, the definition of equation of state for both phases is important. The equation of state which is widely employed is the so - called stiffened gas equation of state, which can describe both gas and liquid phases. The total energy per unit of volume is:

$$E = \frac{p + \gamma B}{\gamma - 1} + \frac{1}{2}\rho u^2 \quad (4)$$

where γ and B for water are $\gamma=7.415$ and $B=296.3$ MPa respectively. When this equation is used for gases, B is zero and γ is the usual specific heat ratio of the individual gases, for instance, for air it is $\gamma = 1.4$. Here an approximate Riemann solver was modified to incorporate the stiffened gas equation of state and the level set approach. The proposed solver is based on that of Mulder et al. [6].

2.3 Interface correction step

The interface correction step is based on concept proposed by Cocchi et al. [1]. The main idea of this approach is that the two grid points positioned in front of and behind the interface are recalculated in the corrector step; thus, a sharp density gradient is maintained. This is done by interpolating the results of the exact Riemann solver at the interface with results obtained from the grid points across the interface that have not been affected by diffusion. Further details regarding the numerical scheme can be found in Igra and Takayama [2].

2.4 Governing equations

The governing equations for compressible inviscid flow in two-dimensional conservation form are:

$$U_t + F_x + G_y = 0$$

$$U = \begin{bmatrix} \rho \\ \rho u \\ \rho v \\ E \end{bmatrix}, \quad F(U) = \begin{bmatrix} \rho u \\ \rho u^2 + p \\ \rho uv \\ u(E + p) \end{bmatrix}, \quad G(U) = \begin{bmatrix} \rho v \\ \rho uv \\ \rho v^2 + p \\ v(E + p) \end{bmatrix} \quad (5)$$

These equations are solved by using an operator splitting technique along with solving the equation of state and the level set function. Thus solving a system of one dimensional equations and employing this method for two-dimensional flow fields as a series of one dimensional problems while retaining the previously described interface correction scheme.

3 Results and discussion

3.1 Experimental setup

Details regarding the experimental setup can be found in Igra and Takayama [3]. Where the process of deformation and breakup of a water column subjected to shock wave loading was visualized using double exposure infinite fringe holographic interferometry.

3.2 Shock wave interaction with a water column

The interaction of a planar shock wave of Mach number 1.3 in air with a water column having an initial dia. of 6.4 mm is numerically simulated using an upwind TVD scheme with the interfacial correction. The initial conditions of the flow field are described in Fig. 1. The corresponding Weber and Reynolds numbers for these conditions are 3,690 and 95,300, respectively. The CFL number is 0.9 and a minmod limiter was used.

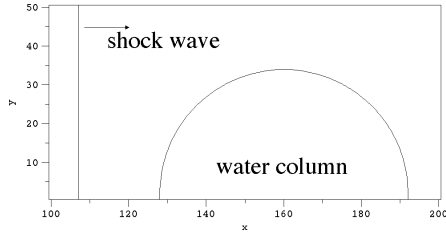


Fig. 1. Schematic diagram of initial conditions of the numerical simulation

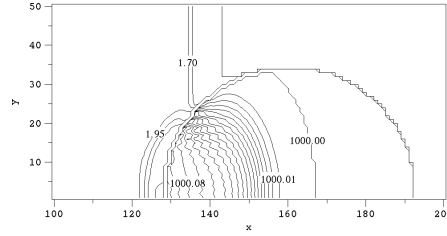


Fig. 2. Isopycnics at $t=2 \mu s$

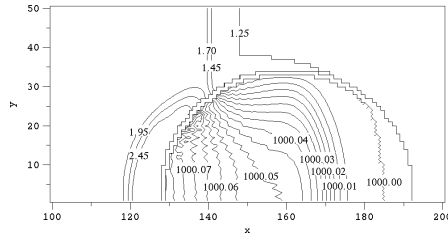


Fig. 3. Isopycnics at $t=4 \mu s$

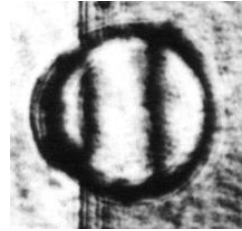
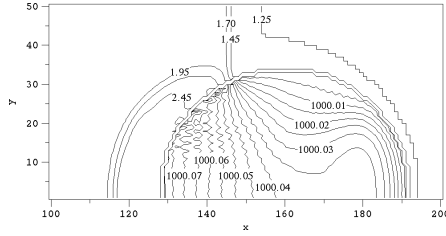
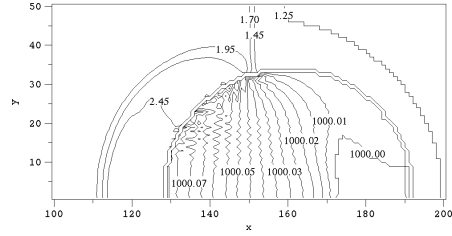
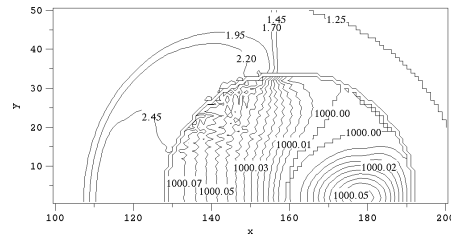
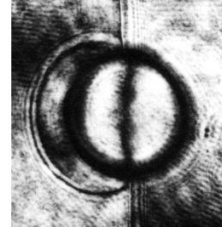


Fig. 4. Experimental interferogram at $t=4 \mu s$

Employing the upwind TVD scheme, the initial stages of the shock wave impingement upon the water column are simulated on a uniform grid of 400×150 points, with 64 grid points located along the water column diameter. The isopycnics at about $2 \mu s$ after the incident shock wave impingement on the water column are shown in Fig. 2. At first a regular reflection appears. It is confirmed for the first time that a transmitted wave appears inside the water column, it propagates faster than the shock wave in air. This is attributed to the higher speed of sound in the water. Due to the large acoustic impedance mismatch between air and water only a fraction of incident shock wave energy is transmitted to the water column. Therefore, the transmitted wave in the water column is a compression wave.

The isopycnics at about $4 \mu s$ after the incident shock wave impinged upon the water column are shown in Fig. 3. Now the reflected shock wave in air is reaching its transition from regular to Mach reflection. The compression wave inside the water column already propagated more than half way inside the water column. It appears to have widened to encompass the whole water column. Figure 4 shows the corresponding experimental interferogram. Shock waves and the gas/liquid interface are clearly observable. The shock wave location appears to be similar to its location in the isopycnics of Fig. 3. Two fringes are observable inside the water column. The first one is near the frontal part of the water column where the high density region corresponds to high pressure, while the second one is slightly curved towards the direction of propagation is nearly in the middle.

Numerical isopycnics at $5 \mu s$ after the incident shock wave impingement are shown in Fig. 5. Now the transmitted shock wave has reached the rear side of

Fig. 5. Isopycnics at $t=5 \mu s$ Fig. 6. Isopycnics at $t=6 \mu s$ Fig. 7. Isopycnics at $t=7 \mu s$ Fig. 8. Experimental interferogram at $t=7 \mu s$

the water column. At the frontal area of the water column a high density region is observed. At this point it is possible to divide the water column into two parts, front and rear. The high density which corresponds to high pressure at the front of the water column is a direct result of the high pressure generated by the reflected shock wave in air. Whereas the density distribution at the rear of the water column is affected by the wave motions of the transmitted shock wave.

Isopycnics at one micro second later are shown in Fig. 6. It is clear from this figure that the transmitted compression wave (inside the water column) is reflected from the air/water interface and becomes an expansion wave. As a result the density at the rear of the water column decreases. At the same time high density region in the front of the water column expands towards the rear, now occupying more than half the area of the water column.

It is seen in Fig. 7 that the front of the high density region is pushed upstream due to the expansion of the high density region observed at the rear of the water column. The region of high density, at the rear of the water column, was generated due to the propagation of the high density region, observed in Fig. 6, towards the column rear end. Thereby compressing the fluid in the rear end of the water column until the current situation is reached. The experimental interferogram corresponding to this condition is shown in Fig. 8, where a single fringe is visible dividing the two high density regions of the water column. There appears to be good agreement between the experimental and the numerical results.

As previously described the interaction of these waves creates a two - dimensional complex waves system. With elapsing time the wave interaction inside the water column becomes more complex while the wave intensity decreases.

During the shock wave interaction described so far the water column has not deformed from its original shape. The shock wave reflection and transition in air appear to be similar to those encountered in shock wave diffraction over a solid cylinder. Therefore it can be concluded that at this early stage of shock wave interaction with a water column the flow field resembles that of shock wave diffraction over solid cylinder. Once the water column begins to deform these similarities will end.

4 Conclusions

As is clearly evident from the numerical results, the proposed scheme is suitable for handling gas/liquid interfaces. It does not create pressure oscillation nor density diffusion at the interface. The interface was captured using the level set approach which was added to a system of conservation laws. A correction scheme based on Cocchi et al. [1] was used. It was modified and employed with the level set approach and a moving interface. Using this numerical scheme the initial stages of a planar shock wave interaction with a water column were studied both experimentally and numerically. Complex wave motions were observed inside the water column. The transmitted wave has propagated back and forth inside the water column. The flow field around the water column is initially similar to that of shock wave interaction with a solid cylinder. Similarity terminates when the interfacial instability appears.

References

1. J. P. Cocchi, R. Saurel, J. C. Loraud: Shock Waves **5**, 347 (1996)
2. D. Igra, K. Takayama: submitted to Int. J. for Numerical Methods in Fluids
3. D. Igra, K. Takayama: Atomization and Sprays, **11**, 167 (2001)
4. D. D. Joseph, J. Belanger, G. S. Beavers: Int. J. of Multiphase Flow **25** 1263 (1999)
5. S. Karni: J. of Comp. Phys. **112** 31 (1994)
6. W. Mulder, S. Osher, J. A. Sethian: J. of Comp. Phys. **100** 209 (1992)
7. A. A. Ranger, J. A. Nicholls: AIAA Journal **7** 285 (1969)
8. J. A. Sethian. Level Set Methods and Fast Marching Methods. Edited by P.G. Ciarlet, A. Iserles, R. V. Vohn and M.H. Wright, Cambridge Monographs on Applied and Computational Mathematics. Cambridge: Cambridge University Press, (1999)
9. A. Wierzba, K. Takayama: Institute of High Speed Mechanics, Tohoku University, (1987)
10. T. Yoshida, K. Takayama: J. of Fluids Eng. **112** 112 481 (1990)